EXPERIMENTAL AND NUMERICAL INVESTIGATION OF A SIMPLIFIED EXHAUST MODEL

Balázs Vehovszky[1,*], Tamás Jakubík[1], Martin Schuster[2]

[1] Department of Whole Vehicle Engineering, Audi Hungaria Faculty of Vehicle Engineering, Széchenyi István University, Egyetem tér 1, 9026 Győr, Hungary
[2] Whole Vehicle Development, Audi Hungaria Motor Kft., Kardán utca 1, 9026 Győr, Hungary

[*] corresponding author: e-mail: vehovszky.balazs@sze.hu

Resume

A simplified experimental equipment was built to investigate heat radiation and free convection around hot exhaust pipe. Temperatures were measured on the surface of the pipe as like as on heat insulating and -reflecting aluminum shield. Special care was taken to the temperature measuring method: result proved that inappropriate fixing of measuring thermocouples lead to an error of up to 30 % in the temperature-increase values. A detailed 1D numerical model was set up and parametrized so as to the calculation results can be fitted to measured temperature values. In this way thermal properties of the surfaces – as emissivities, absorption coefficients and convective heat transfer coefficients – were determined for temperature sweeps and stationary state cases. The used methods are to be further improved for real automotive parts and higher temperatures.

Available online: http://fstroj.uniza.sk/journal-mi/PDF/2016/13-2016.pdf

1. Introduction

Large Heat flow around vehicle exhaust system is of great importance as regards heat insulating and other elements nearby hot parts. Experimental results as like as numerical simulations are commonly used to handle thermal effects [1, 2]; however, the results of these examinations are not always consistent. Inaccurate radiation settings in the numerical model and erroneous estimation of free convection are among the most usual reasons of this delusion [3].

Regarding real in-vehicle operation, the overheating of exhaust heat reflecting shield and nearby elements during heavy duty operations can be the consequence of an improper heat design. The risk of this malfunction is extremely increased when the combination of high exhaust temperature (due to e.g. high engine performance)

with low forced flow (i.e. low vehicle speed) occurs. Such conditions can come up for example when the car stops immediately after a forced highway run, or during pulling heavy load uphill [4]. Dirt on the heat reflecting elements or extreme ambient conditions (e.g. hot black asphalt) further increases the chance of exhaust system overheating.

To handle this issue, well-harmonized experiments and numerical simulations should be executed. During our work we targeted the investigation of an in-between area: a simple model measurement, which could be effectively parametrized for real conditions and accurately simulated numerically. The two most unsettled processes: the heat radiation and the free convection are in the focus of our research, which were examined via experimental and numerical methods.

2. Experiments

A simplified exhaust tube – heat reflecting shield setup was designed and built aiming the effective modelling of heat transfer processes. The equipment consists of a part of an exhaust tube (stainless steel, OD Ø54 mm) with its fittings, a hot air supply (Steinel 3483 heat gun, up to 650°C air temperature), a half cylinder-shape aluminum heatshield (Ø220 mm) with 30 mm rock wool outer insulation and 23 temperature measurement points (K-type thermocouples, 4×3 on the tube – marked with red dots, 3×3 on the heatshield – marked with blue dots and 2 inside the tube for measuring heating air temperature – marked with hollow orange dots, see Fig. 1). Three main sections along the tube were defined: the inflate side has the highest

temperature while the outlet has the lowest.

During the design of the apparatus special care was taken to:
- Hot air inlet to exclude ambient temperature suck (resulting cooler tube);
- Fixing of hot elements to minimize heat transfer via conduction (using heat resistant rubber and silicone fixtures);
- Fixing the thermocouples:
  o Air temperature was measured with coaxial, hermetically insulated ones
  o Tube surface temperature was measured with spot-welded thermocouples
  o Thermocouples on the aluminum heatshield (inner side) were fixed by aluminum adhesive tape – the effect of fixing method was also investigated.

a) layout
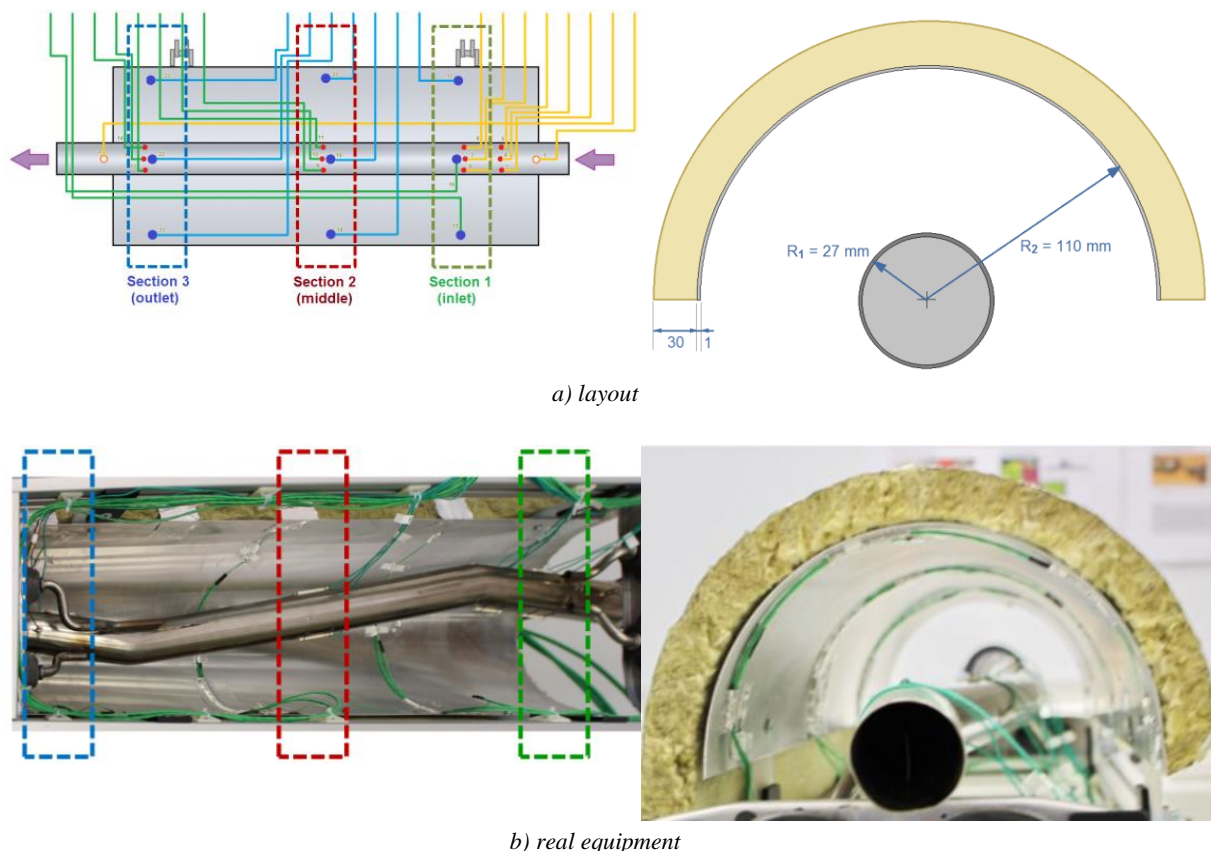
b) real equipment
Fig. 1. The measurement scheme.
(full colour version available online)

Basic measurement course was started at ambient temperature for all parts of the apparatus. During continuous registration of the temperatures the heat gun was switched on and the tube started to heat up; meanwhile the heatshield warms up too due to heat radiation and convection. After around 1 hour the temperature of the system becomes stationary resulting a ΔT_G, ΔT_T and ΔT_S temperature excess compared to ambient temperature for the gas, the tube and the heatshield, respectively (see Fig. 2).

For being able to investigate the effect of thermal convection and heat radiation separately, the apparatus was designed for operation in normal and upside-down (inverted) position too. Latter one excludes heat convection from the exhaust tube → heatshield heat transfer path (see Fig. 3).

The effectiveness of heat flow (thermal convection) elimination during inverted setup measurement was proven by measuring the temperature of the heatshield surface and the air temperature just above the heatshield (see Fig. 4). If considerable heat flow occurs between the tube and the heatshield, the air temperature would be higher than that of the surface (the air would heat the shield). In contrast, air temperature was equal or slightly below the shield surface temperature, which proves that no significant heat flow via air occurs between the tube and the heatshield (practically, the shield warms up the air above itself).

Taking into account the above considerations, one can conclude that in the reversed position the only heat transfer path from the heated tube to the heatshield is thermal radiation. Thus, at this setup mode the clear radiation properties can be examined concerning the heat input of the heatshield. Furthermore, comparing the results of normal and inverted position measurements, the impact of free thermal convection on the warming of heatshield can be calculated.

Aiming the investigation of different surface qualities, two modifications of the aluminum heatshield inner side were tested beside the base (as-rolled aluminum sheet) surface (see Fig. 5):

− Modification of roughness: polished and roughened with sandpaper (P120 grit);
− Modification of color: coated with black (Kontakt Chemie Graphit 33) and white (MR Chemie MR 70 developer white) sprayed layer;

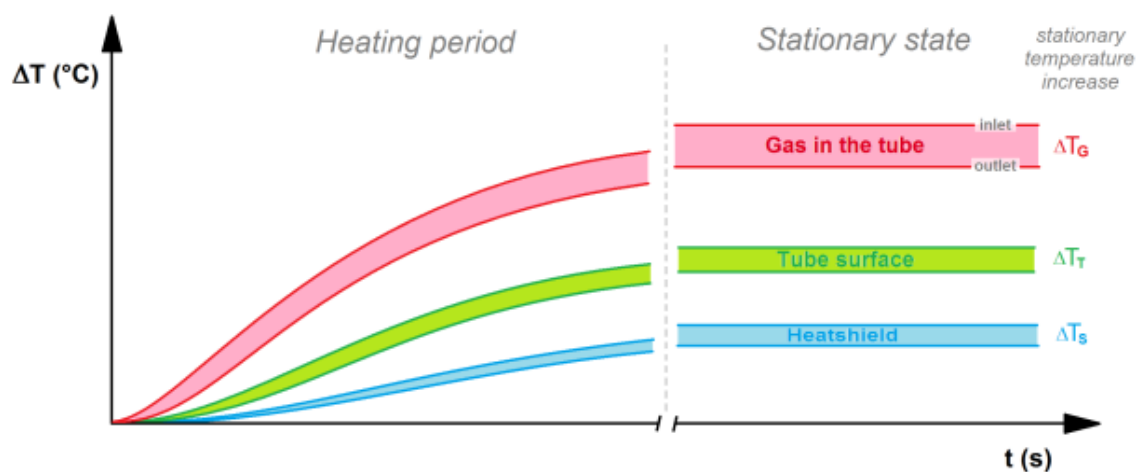The surface color modification of exhaust tube was also investigated.

Fig. 2. The characteristic temperature increase of the gas (ΔT_G), the tube (ΔT_T) and the heatshield (ΔT_S) during heating up and in stationary state.
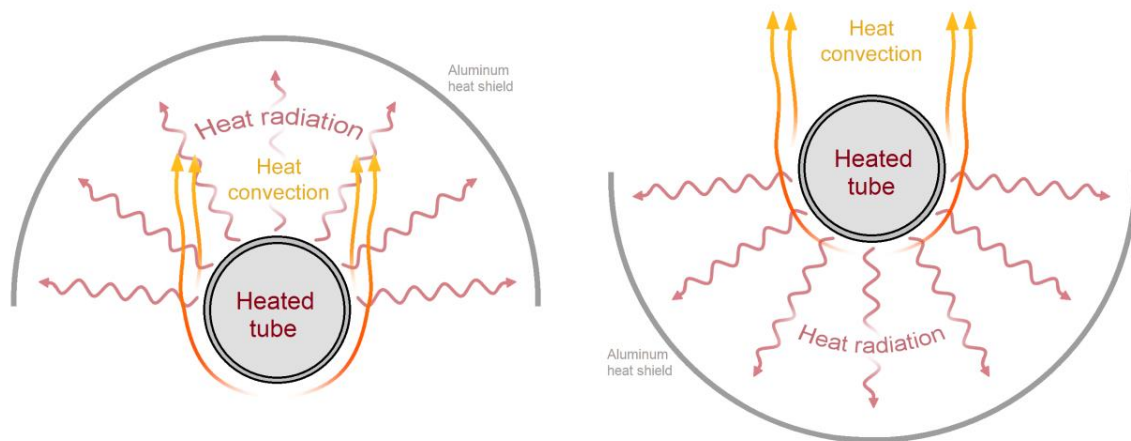
(full colour version available online)

Fig. 3. Heat transfer from tube to heatshield at normal (left) and inverted (upside-down, right) position.
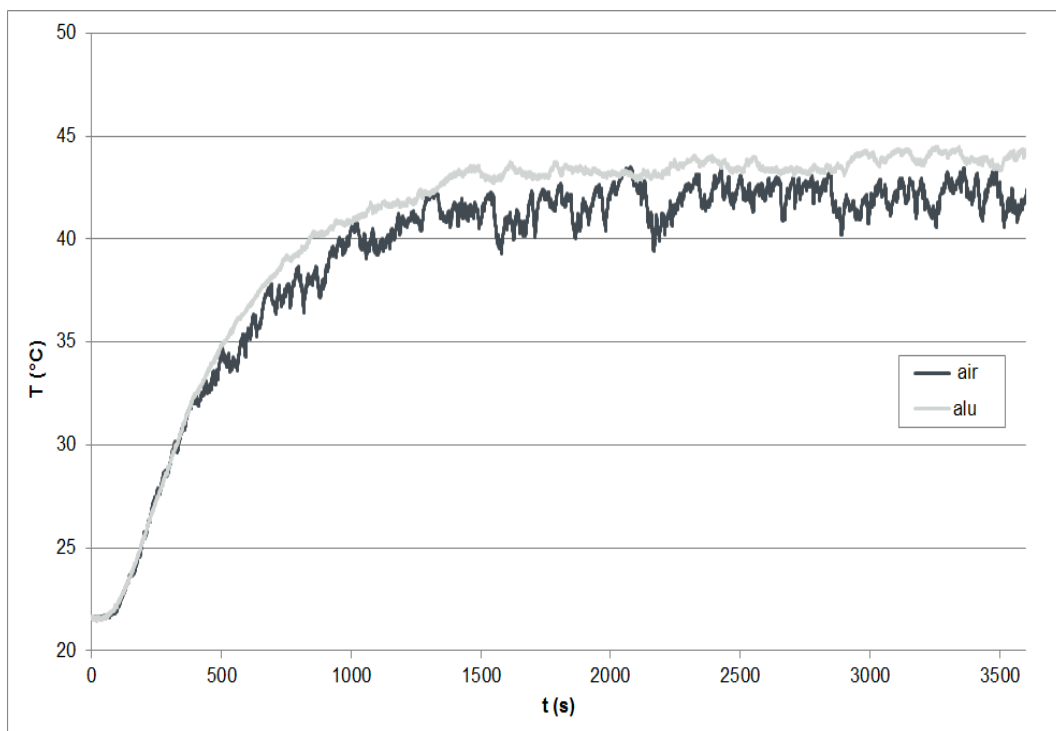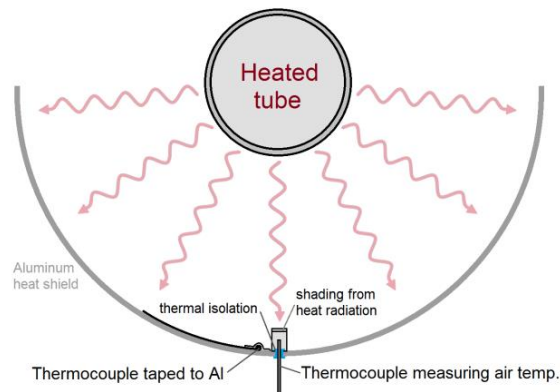*(full colour version available online)*

Fig. 4. Temperature measurement at inverted position proved the absence of heat flow from the tube.
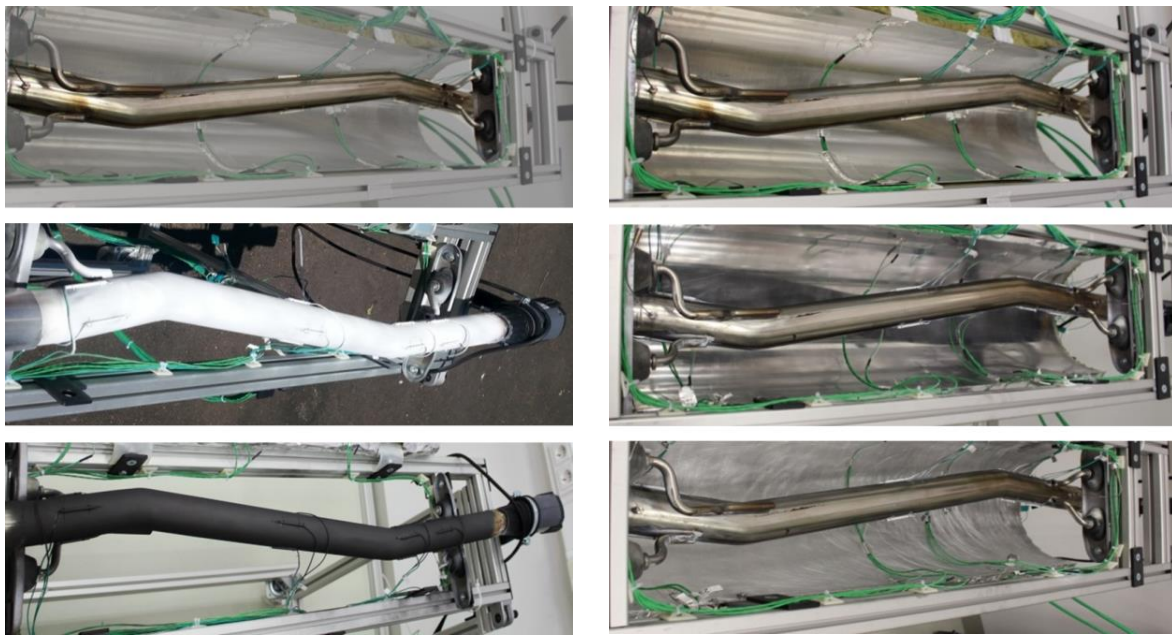*(full colour version available online)*

Fig. 5. Different surface colours of the tube (left) and roughness of heatshield (right).
(full colour version available online)

As mentioned previously, the sticking method of thermocouple onto aluminum heatshield surface was also investigated, as even such a simple temperature measurement method can result in erroneous values [5]. Sticking thermocouples with aluminum adhesive tape onto aluminum heatshield surface was proved to be the best solution. The detailed description of this examination could not be presented in this work.

Our goal in the following is – after ensuring the high precision of measurements – to examine experimentally the heating up of the heatshield at inverted position beside different surface conditions, and reproduce the measured values with a 1D numerical model. By fitting the model results to the measured values, the parameters of the model (emissivities, absorption and convective heat transfer coefficients) will be determined.

3. Theoretical considerations and numerical model

In the first step let's focus on thermal radiation. The basic principle is stated by the Stefan-Boltzmann law (1) which gives the eradiated thermal energy [6]:

$$\dot{Q} = \varepsilon \cdot \sigma \cdot T^4 \cdot A \tag{1}$$

where $\dot{Q}$ denotes the radiated heat flux, ε is the emissivity, T is the absolute temperature and A is the surface area of the radiating body. The absorbed radiation power can be given as equation (2):

$$\dot{Q}_{abs} = \alpha \cdot \dot{Q}_{inc} \tag{2}$$

where $\dot{Q}_{inc}$ is the overall incident radiation and α is the absorption coefficient. According to Kirchhoff's law, the emissivity (ε) and the absorption coefficient (α) are equal for a given surface [7].

3.1 Simplified numerical considerations for thermal radiation

For a rough estimation from steady-state temperature increments (ΔT_G, ΔT_T and ΔT_S see Fig. 2) of the tube-heatshield system at inverted position the following considerations

can be established:

- We assume, that the only heat input of the heatshield is the radiation from the heated tube, thus, *the input thermal energy is proportional to the emissivity* of the tube / *absorption coefficient* of the heatshield inner surface. (Heat convection and heat conduction as thermal energy inputs are negligible.)
- Taking into account the low temperature of heatshield at inverted setup (generally 5-20 degrees above room temperature) its heat loss via radiation is negligible compared to other het loss modes. As both free convection and heat conduction are proportional to temperature difference, the *energy loss of heatshield* can be considered as being *proportional to temperature excess* over ambient temperature.
- In steady state the energy loss of heatshield is equal to its energy intake.

Based on the above assumptions, one can conclude, that the temperature increment of the heatshield (ΔT_T) in steady state is proportional to the emissivity of exhaust tube (ε) or absorption coefficient of the heatshield (α) (whichever was changed), see equations (3) and (4):

$$\frac{\Delta T_{T_1}}{\Delta T_{T_2}} = \frac{\varepsilon_1}{\varepsilon_2} \text{ (when } \alpha = \text{const.)} \tag{3}$$

as well as:

$$\frac{\Delta T_{T_1}}{\Delta T_{T_2}} = \frac{\alpha_1}{\alpha_2} \text{ (when } \varepsilon = \text{const.)} \tag{4}$$

This speculation enables us to give a rough estimation to the emissivities and absorption coefficients of different surfaces from the steady-state temperatures at inverted position, however, the preconditions contain some arbitrary simplifications – as the zero thermal radiation of heatshield and the supposition of constant exhaust tube temperature – which shows the limitations of this simplified model.

3.2 Detailed numerical model setup

Aiming the empirical determination of emissivities / absorption ratios of different surface qualities, a 1D numerical model was built up based on elementary thermodynamics and measured data. The temperature of center cross section of heatshield during heating up was calculated parametrically from related measured temperatures and the result were fitted to directly measured temperature values. Parameter values were determined according to best fit (least sum of squares).

The heat transfer processes that were taken into account in the numerical model are visualized in Fig. 6. The calculations were made at inverted position, thus thermal convection from the tube to the heatshield could be neglected.
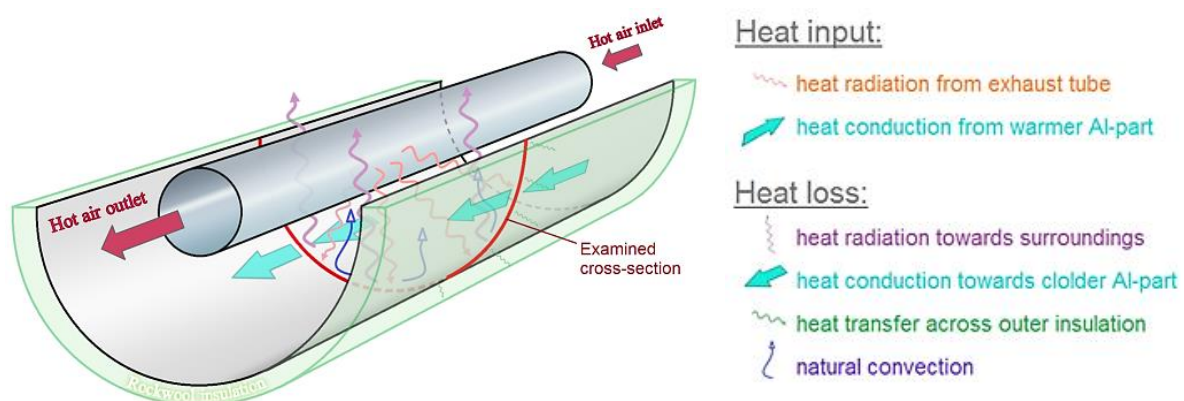

Fig. 6. Thermal components of numerical model.
(full colour version available online)

As the heating of the tube was realized by hot air flow, its temperature is decreasing from the inlet to the outlet. It causes a temperature gradient in the heatshield too.

Heat input of the examined section of the heatshield consists of two components:

1. The thermal radiation of heated tube (irradiation);
2. Heat conduction inside the heatshield from its warmer side.

Heat loss consists of the following components:

1. Thermal radiation of heatshield (emission);
2. Free convection of warmed air;
3. Heat transfer toward outer insulation;
4. Heat conduction toward cooler side of the heatshield (hot air outlet side).

Radial direction heat gradient in the heatshield can be neglected as its width is small (1 mm) and aluminum has excellent thermal conductivity (205 $W \cdot m^{-1}K^{-1}$ [8]). The temperature of heatshield middle line is considered to be constant too – meaning no heat flow in tangential direction. Temperature values for calculation and validation are get from the bottom (center) line of the heatshield.

Practically, the following measured data were used during calculation:

– Ambient temperature;
– Temperature of exhaust tube surface middle (bottom) point at the middle cross section for heat irradiation;
– Temperature of heatshield surface middle (bottom) point at inlet and outlet cross section for heat conduction inside the heatshield in axial direction;
– For parameter fitting, the calculated temperature values of heat shield examined cross section were fitted to measured temperatures at its surface middle (bottom) point at middle cross section during heating up;
– The calculated instantaneous temperature of heatshield middle (examined) cross section

was used for the calculation of all other heat transfer modes.

The parameters which were determined via fitting:

– Emissivity of exhaust tube ($\varepsilon_{tube} = \alpha_{tube}$) beside different surface conditions (as-received, sprayed black and sprayed white);
– Absorption coefficient of heatshield ($\alpha_{shield} = \varepsilon_{shield}$) beside different surface conditions (as-rolled, sprayed black, sprayed white, polished and roughened);
– Convective heat transfer coefficient of heatshield (kc or sometimes marked as h) for free convection beside different surface conditions (as-rolled, sprayed black, sprayed white, polished and roughened).

Thermal conductivity of aluminum heat shield (k_{Al}) and heat transfer coefficient of rock wool insulation (k_{ins}) were taken from literature [8, 9].

3.3 Calculation of radiation

Thermal conduction, heat transfer trough insulation and free convection were calculated according to well-known governing equations [6]. Heat radiation calculation, however, is a bit more difficult, as:

1. Emitted radiation by one part irradiates the other part at a proportion of view factor.
2. Incident radiation is partly reflected and after reflection(s) it can reach the surface again.

View factors at a pipe-half pipe setup can be determined as shown in Fig. 7. [10]
Using the data of current case, we get:
$r = 0.2455 = F_{21}$; $F_{22} = 0.3441$; $F_{23} = 0.4104$.

Multiple reflections of heat radiation are of interest when calculating radiated thermal energy from exhaust tube to heatshield and the amount of emitted thermal energy by heat shield – partly backscattered by exhaust tube. To deal with this issue, the *apparent absorption coefficient (α_{shield}^{app})* of the heatshield

is introduced, meaning the ratio of overall absorbed radiation relative to irradiation. Hereinafter heat emission toward surrounding is considered as heat loss – supposing large enough space to neglect reflections, and thermal heat transmission is set to zero for each part – thus the whole irradiation goes to absorption or reflection.

Start the consideration with the amount of heat reaching the inner surface of heat shield (considered as being uniformly dispersed): Q_0 – see Fig. 8a. According to eq. (5) the amount of direct absorption equals:

$$Q_{abs1} = Q_0 \cdot \alpha_{shield} \tag{5}$$

while first reflection is given by eq. (6):

$$Q_{ref1} = 1 - Q_{abs1} = Q_0 \cdot (1 - \alpha_{shield}) \tag{6}$$

Supposing uniform reflection and using equations of Fig. 7 the backscattered radiation that reaches the central tube can be given as (7) (see Fig. 8b):

$$Q_{ref1}{}^{tube} = F_{21} \cdot Q_{ref1} = F_{21} \cdot Q_0 \cdot (1 - \alpha_{shield}) \tag{7}$$

while the backscattered radiation that reaches the heatshield again (8) equals:

$$Q_{ref1}{}^{shield} = F_{22} \cdot Q_{ref1} = F_{22} \cdot Q_0 \cdot (1 - \alpha_{shield}) \tag{8}$$

The backscattered radiation towards surroundings has no relevance for us – as mentioned above.

The amount of re-reflected radiation by tube is given by (9):

$$Q_{re-ref1}{}^{tube} = (1 - \alpha_{tube}) \cdot Q_{ref1}{}^{tube} \tag{9}$$

One problematic point is that the re-reflected radiation by tube surface ($Q_{re\text{-}ref1}{}^{tube}$)

is not dispersed uniformly to all directions (see Fig. 8/c): most of the re-reflected heat is directed backward to heatshield ($Q_{re\ ref1}{}^{tube \rightarrow shield}$) and only a smaller part is oriented to the surroundings. This ratio depends e.g. on the surface roughness (via the rate of scattering compared to straight reflection). To handle this effect we assume homogenous scattering by heatshield and suppose: that part of re-reflection is directed back toward the heatshield which reaches the bottom side of the tube – as marked in Fig. 9. Based on the indicated geometries and incident radiation surface distribution, the ratio of re-reflected radiation toward heatshield compared to the whole amount of re-reflected radiation (considered as the reflection-efficiency of the tube toward the heatshield) can be expressed as (10) (where $r = R_{tube}/R_{shield}$):

$$\eta_{tube\_ref} = \frac{Q_{re-ref1}{}^{tube \rightarrow shield}}{Q_{re-ref1}{}^{tube}} =$$
$$= 1 - \frac{\arccos(r)}{4\,(\arccos(r) + \arcsin(r))} \tag{10}$$

Summarizing equations (5) – (10) the re-reflected radiation from the tube to the heatshield can be expressed from the original incident radiation (Q_0) as (11):

$$Q_{re-ref1}{}^{tube \rightarrow shield} = Q_0 \cdot \eta_{tube\_ref} \cdot F_{21} \cdot$$
$$(1 - \alpha_{tube}) \cdot (1 - \alpha_{shield}) \tag{11}$$

Adding the directly reflected radiation which reaches the heatshield directly ($Q_{ref1}{}^{shield}$ see (6) and Figs. 8b and c), the overall heat radiation that was back-reflected to the heatshield during the first reflection step is given by eq. (12) as follows:

$$Q_{ref1}{}^{shield\ ovarall} = Q_0 \cdot (1 - \alpha_{shield}) \cdot$$
$$(\eta_{tube\_ref} \cdot F_{21} \cdot (1 - \alpha_{tube}) + F_{22}) \tag{12}$$
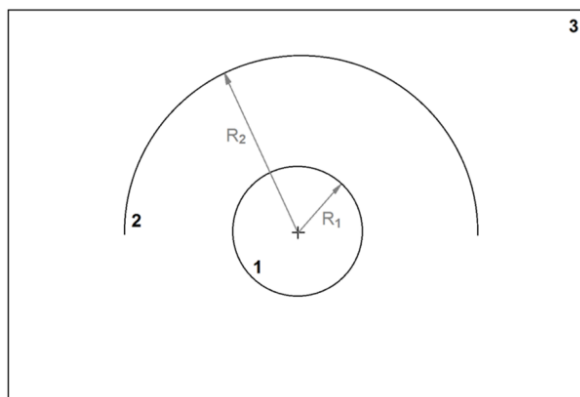
F_{xy} is the view factor of the radiation from x incident on y:

$r = R_1/R_2$
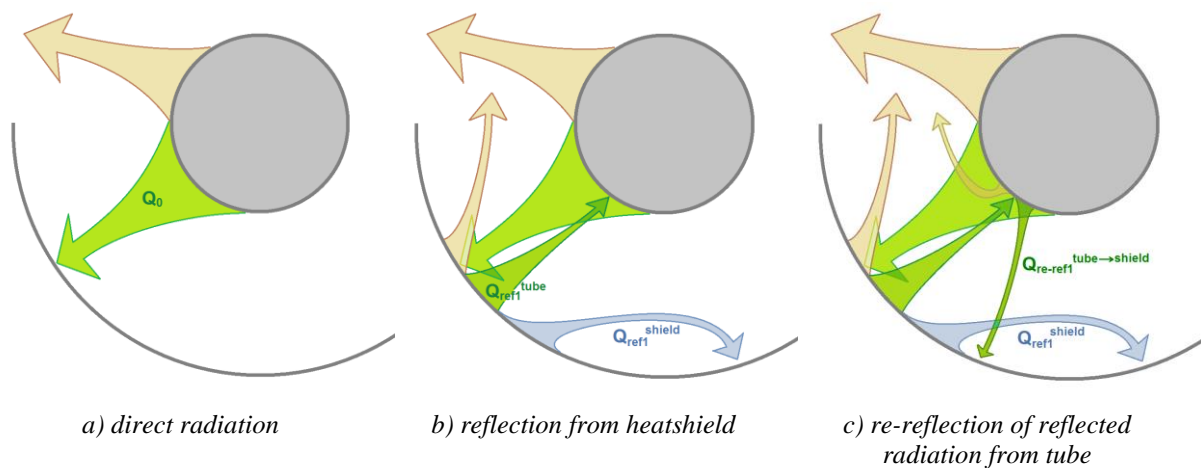
$F_{12} = F_{13} = 0.5$

$F_{21} = r$

$F_{22} = 1 - \frac{2}{\pi}\left(\sqrt{1-r^2} + r \cdot sin^{-1}r\right)$

$F_{23} = 1 - F_{21} - F_{22}$

Fig. 7. View factors of a tube – half-tube setup.

a) direct radiation   b) reflection from heatshield   c) re-reflection of reflected radiation from tube

Fig. 8. Reflection of tube thermal radiation.
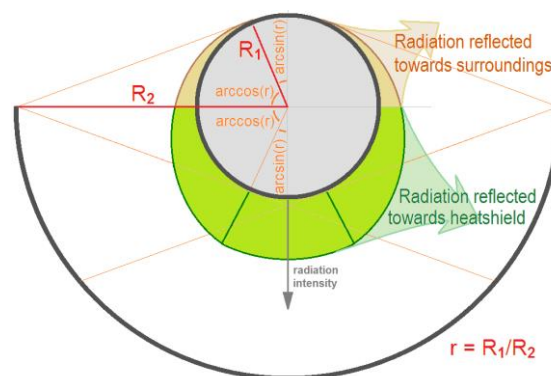(full colour version available online)

Fig. 9. Distribution of the radiated heat comes from the heatshield and back-reflected by the tube.
(full colour version available online)

Substituting original incident radiation (Q_0) by the overall first reflection we can get the amount of radiation that was backscattered to the heatshield in the second reflection step analogously. In general, the amount of radiation that was backscattered to the heatshield after the nth reflection step can be written as (13):

$$Q_{refn}^{shield\ ovarall} = Q_0 \cdot \Big((1 - \alpha_{shield}) \cdot (\eta_{tube\_ref} \cdot F_{21} \cdot (1 - \alpha_{tube}) + F_{22})\Big)^n \qquad (13)$$

Consequently, the radiation that is absorbed by the heatshield after the nth reflection step is given by equation (14):

$$Q_{abs}^{n^{th}step} = \alpha_{shield} \cdot Q_0 \cdot \left((1 - \alpha_{shield}) \cdot (\eta_{tube\_ref} \cdot F_{21} \cdot (1 - \alpha_{tube}) + F_{22})\right)^n \quad (14)$$

The overall absorbed radiation is the sum of absorbed amounts in each step – see (15):

$$Q_{abs}^{overall} = \sum_{i=0}^{\infty} \alpha_{shield} \cdot Q_0 \cdot \left((1 - \alpha_{shield}) \cdot (\eta_{tube\_ref} \cdot F_{21} \cdot (1 - \alpha_{tube}) + F_{22})\right)^i \quad (15)$$

Mathematically it is the sum of a geometric series, which can be written simply as equation (16):

$$\sum Q^{shield} = \frac{\alpha_{shield} \cdot Q_0}{1 - (1 - \alpha_{shield}) \cdot (\eta_{tube\_ref} \cdot F_{21} \cdot (1 - \alpha_{tube}) + F_{22})} \quad (16)$$

We can finally express a so-called **apparent absorption coefficient** of the heatshield – given by eq. (17):

$$\alpha_{shield}^{app} = \frac{\alpha_{shield}}{1 - (1 - \alpha_{shield}) \cdot (\eta_{tube\_ref} \cdot F_{21} \cdot (1 - \alpha_{tube}) + F_{22})} \quad (17)$$

which is the ratio of the total absorbed radiation by the heatshield and the initial incident radiation.

Hereinafter, the heat absorption can be calculated from the incident radiation using apparent absorption coefficient – which incorporates all further reflections. This method simplifies calculations, thus makes parameter fitting faster and easier.

As one can see, the apparent absorption coefficient depends on the absorption coefficients of the heatshield and the tube, on the geometry trough view factors (F_{21} and F_{22}) and on the reflection efficiency (η_{tube_ref}) – latter is also a geometry-dependent variable, but surface characteristics)as e.g. diffusivity

of reflection) can also be incorporated into this parameter.

If we calculate the apparent absorption coefficient for different surfaces, we can see that it can be more than twice of the real absorption coefficient of the heatshield when both the heatshield and the exhaust tube own low absorption coefficient (high reflectivity). On the other hand, if exhaust tube is considered as a black body, $\alpha_{shield}^{app} / \alpha_{shield}$ ratio falls into the 1...1.52 range – higher values correspond to higher reflectivity of the heatshield, resulting stronger *heatshield → heatshield* reflections.

The energy loss of heatshield via thermal radiation was handled in a similar manner: substituting Q_{refl} by the thermal heat emission of heatshield, all further considerations and calculations concerning reflections can be treated in the same way as described above.

3.4 The numerical model

The numerical model was built up along the previously described principles: the overall heat balance of the heatshield middle line was constructed. The base equation (18) declares the balance of input-, egressed and stored energies (heat amount per unit time) per unit mass:

$$\Delta\dot{E} = \dot{Q}_{input} - \dot{Q}_{output} \quad (18)$$

where ΔE denotes the stored thermal energy via temperature increase (heat capacity).

Explicating the components of (18) equation (19) is resulted:

$$C_{p\,Al} \cdot \Delta\dot{T}_S = \dot{Q}_{cond}^{tot} + \dot{Q}_{rad}^{tot} - \dot{Q}_{ins} - \dot{Q}_{conv} \quad (19)$$

with the nomenclature:

  Q_{cond}^{tot}: Total heat input energy via heat conduction of heatshield aluminum (heat input from warmer side minus heat output toward cooler side of heatshield)

Q_{rad}^{tot}: Total radiated energy input (irradiation from exhaust tube minus thermal emission by shield);

Q_{ins}: Heat loss trough outer insulation of the heatshield;

Q_{conv}: Heat loss via free convection;

$C_{p\,Al}$: The specific heat capacity of aluminum (heatshield material);

$\Delta\dot{T}_S$: The rate of temperature-increase of heatshield.

Numerical model was based on equation (19) with a time step of 0.5 s and total heating time of 3600 s.

The values (parameters, constant and measured values) that were used during calculations are listed in Table 1.

The numerical model was built up in Microsoft Excel with a time step equal to measurement (0.5 s). After giving initial values (given in Table 1. in braces after each variable) the variables were optimized so as to reach minimum difference (sum of squares) between measured and calculated temperature values of heatshield at examined point. To compensate the high number of measured values at stationary state compared to that of heating ramp, relative differences were used for the fitting – normalized by temperature increase relative to initial temperature.

Optimization processes were executed by Solver module using nonlinear GRG (gradient) method using adjacent differences and 10^{-4} convergence criterion.

Table 1

List of numerical values used for calculation.

Name / Description	Notation	Value
Constants – Geometrical properties		
Radius of heated tube	R_1	0.027 m
Radius of heatshield	R_2	0.11 m
Distance of sections 1 and 3 from the middle section	-	0.28 m
Heatshield insulation thickness	-	0.03 m
Heatshield aluminum sheet thickness	-	0.001 m
Calculated view factors from the setup's geometry	-	see Fig. 7.
Constants – Thermal and physical properties		
Conductivity of aluminum	k_{Al}	205 W.mK^{-1}
Specific heat capacity of aluminum	C_p	897 J.kg^{-1}.K^{-1}
Density of aluminum	ρ_{Al}	2700 kg.m^{-3}
Stefan-Boltzmann-constant	σ	$5.67 \cdot 10^{-8}$ W.m^{-2}.K^{-4}
Variables – Emissivity and convective heat transfer coefficient of different surfaces (values given in brackets are initial values of parameter fitting according to [11])		
Emissivity of as-received exhaust tube	ε	(0.5)
Emissivity of black-sprayed exhaust tube	ε	(0.97)
Emissivity of white-sprayed exhaust tube	ε	(0.6)
Emissivity of as-rolled aluminum heatshield	ε	(0.09)
Emissivity of black-sprayed aluminum heatshield	ε	(0.8)
Emissivity of white-sprayed aluminum heatshield	ε	(0.6)
Emissivity of roughened aluminum heatshield	ε	(0.2)
Emissivity of polished aluminum heatshield	ε	(0.06)
Convective heat transfer coefficient of as-rolled heatshield	k_c	(5)
Convective heat transfer coeff. of white coated heatshield	k_c	(5)
Convective heat transfer coeff. of black coated heatshield	k_c	(5)
Convective heat transfer coeff. of roughened heatshield	k_c	(10)
Convective heat transfer coeff. of polished heatshield	k_c	(5)
Measured values		
Ambient temperature (for the calculation of emitted heat of heatshield)		
Temperature of exhaust tube surface middle point at middle section (above examined heatshield area, for radiated heat calculation)		
Temperature of heatshield at the inlet and at the outlet section (for conducted heat input and output calculation)		

4. Results and discussion

As described above, exact surface thermal radiation and convection properties were determined by fitting numerical model (described in Chapter 3.2) to measured temperature data. To illustrate this method, two results were shown in Figs. 10 and 11 - for base (unmodified) surfaces and for black coated tube and heatshield surfaces, respectively. Despite the not totally accurate fit, the typical difference of measured and calculated values does not exceed 0.2°C, the standard deviation of relative error is 0.04 for the unmodified surfaces (keep in mind the logarithmic axis of temperature!). The situation of black tube and black heatshield is even better: in this case the fitting follows quite

accurately the measurements: typical difference of measured and calculated values are within 0.1°C, the standard deviation of relative error is 0.01.

The accuracy of fitting depends mostly on the reflectivity of the surfaces: the model describes most accurately the homogenously scattering, highly absorbing surfaces (with lower ratio of reflection).

As described above, calculation fitting was executed via parameter optimization resulting refined values of emissivities, absorption coefficients and convective heat transfer coefficients (of heatshield) for different surfaces. However, due to industrial secret, direct numerical data could not be presented in this paper.
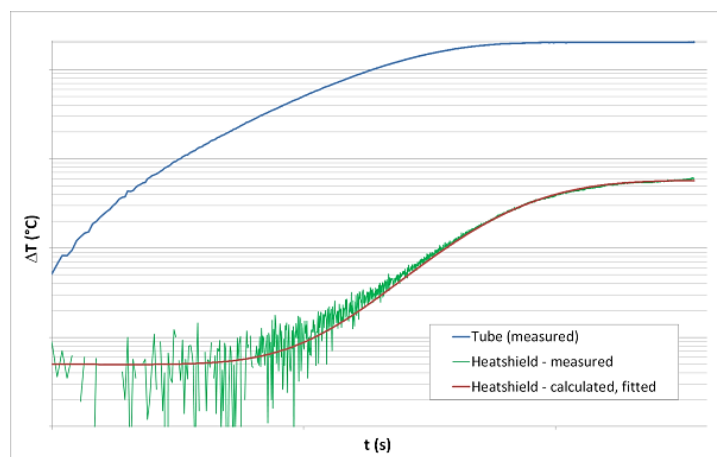

Fig. 10. Measured and calculated temperature data of tube and heatshield – both with as-received surface.
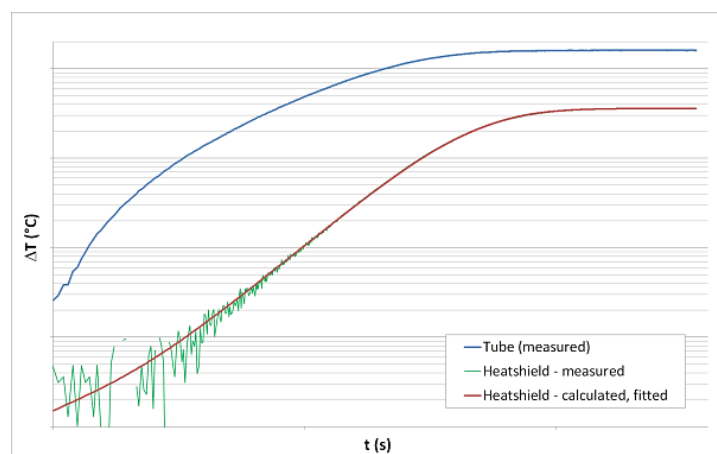*(full colour version available online)*

Fig. 11. Measured and calculated temperature data of tube and heatshield – both with black coated surface.
(full colour version available online)

5. Conclusions

A simplified setup of car exhaust tube – heat shield system was designed and built. Using this equipment different aspects of heat transfer processes were investigated. Heat radiation and free convection were set in the focus; their effects were uncoupled by using the system in upside-down (inverted) position. A simplified theory was developed for rough estimations from steady state temperatures of the system, as like as a more complex numerical model was built up aiming the determination of the system's thermal properties via fitting calculated data to measured ones.

The most important findings are:

1. Using well-parameterizable and flexible measurement setup, the thermal radiation and convection effects were successfully decoupled and different surfaces were examined.

2. A detailed numerical model was created, which incorporates heat conduction, convection and radiation too. By introducing apparent absorption coefficient, multiple reflections were handled in a convenient and effective way.

3. The thermal properties of tube and heatshield were determined by fitting the calculation to measurement data via parameter optimization. Low fitting deviation implies that the numerical model was built up in an adequate way. Fitting error and theoretical consideration equally prove that the numerical model gives the best results for highly absorptive/diffusively reflective surfaces – as e.g. porous coatings.

4. Results are usually in good accordance with literature data however, we get slightly different (presumably more accurate) values for some surfaces (e.g. for matte white and black coatings).

5. k_c values for free convection above heat heatshield were also determined, which are in good accordance with expectations.

Considering the results and issues that emerged during examinations the following additional tasks are planned in the near future:

1. Reconstruct the measuring equipment for making it suitable for higher tube-surface temperature (up to 600°C).

2. Thorough examination of free convection in normal setup (heatshield above tube).

3. Measuring on real automotive heatshield (embossed aluminum sheet).

4. Building up CFD and radiation simulation models, which should be developed and validated according to measurements.

References

[1] S. Yang, D. Wang, Y. Dang, L. Li: SAE International (2015), doi: 10.4271/2015-01-2902.

[2] F. Fortunato, M. Caprio, P. Oliva, G. D'Aniello, P. Pantaleone, A. Andreozzi, O. Manca: SAE International (2007), doi:10.4271/2007-01-1094.

[3] A.C. Alkidas, P.A. Battiston, D.J. Kapparos: SAE International (2004), doi: 10.4271/2004-01-0050.

[4] T. Binner, H. Reister, E.P. Weidmann, J. Wiedemann: Aspects of Underhood Thermal Analyses, Progress in Vehicle Aerodynamics IV: Numerical Methods, Tagungsband KFZ-Aerodynamik (Research Institute of Automotive Engineering and Vehicle Engines Stuttgart (FKFS)) 2006.

[5] C. Hochenauer, J. Wurm: Smart Science 2(3) (2014) 116-125.

[6] John H. Leinhard IV and John H. Leinhard V: A heat transfer textbook, Phlogiston Press, Cambridge, Massachusetts, 2008.

[7] Max Planck: The theory of Heat Radiation, P. Blakiston's Son & Co., Philadelphia, 1914.

[8] http://www.engineeringtoolbox.com/thermal-conductivity-d_429.html.

[9] Rockwool datasheet, http://www.rockwool.gr/files/RW-GR/Product%20range/Industrial/Rockwool_Larock%2040%20ALS.pdf.

[10] I. Martínez: Radiative view factors – educational material, Technical University of Madrid, Department of Propulsion and Thermal Fluid Dynamic,http://webserver.dmt.upm.es/~isidoro/tc3/Radiation%20View%20factors.pdf.

[11] http://www.infrared-thermography.com/material.htm